Medical & Biological Engineering & Computing (2022) 60:1815–1825
https://doi.org/10.1007/s11517-022-02576-2

REVIEW ARTICLE

The helical axis of anatomical joints: calculation methods, literature review, and software implementation

Andrea Ancillao[1]

Received: 2 November 2021 / Accepted: 19 April 2022 / Published online: 12 May 2022

Abstract
The calculation of the helical axis, a.k.a. screw axis, is a functional technique that was introduced for the characterization of the motion and the stability of a human joint. Examples are its applications in the design of prostheses and its use for evaluating the joint performance in post-operatory follow-up. The typical way of studying the variations in the helical axis is to instantaneously compare it to some reference. The reference is typically assumed as (i) an anatomical or geometrical reference (e.g., the condyle to condyle axis or an anatomical plane); (ii) a functional reference, i.e., some axis calculated in a functional way. Calculating the helical axis means determining its orientation and its position, based on the recorded motion of the joint. This paper reviewed the calculation methods of the helical axis, its clinical applications, and the most relevant findings. The operative equations of the most common procedures were clearly and synthetically illustrated. More in detail, the focus of this review was set on the calculation of (i) the instantaneous helical axis; (ii) the finite helical axis; (iii) the average helical axis; (iv) a functional coordinate system attached to the helical axis; and (v) the analysis of the time variations of helical axis. The calculation of those quantities was implemented in MATLAB and the code was proposed as supplementary material. The calculation of the discussed quantities was demonstrated on a sample dataset.

Keywords Calculation method · Finite helical axis · Helical axis · Human motion analysis · Human joint · Instantaneous helical axis · Screw axis

1 Introduction

Thanks to the modern motion analysis methods and measurement systems, it is possible to support the clinical practice with quantitative and objective data [1]. Such techniques allow the measurement of several quantities aimed to describe the functionality of joints and ligaments [2, 3] and the body posture during complex motor tasks [4]. For example, it was proven that the healthiness of the human joints (e.g., the knee) and strength/weakness of the ligaments are related to their mobility or stability across a movement [5–8]. This led to the design of clinical motor test and measurements protocols aimed to assess the kinematics and the kinetics of the joints [5, 9–11]. In general, it is possible to represent the motion and the 3D attitude of a joint via several methods. In the clinical practice, the most accepted are the Euler angles or other angular representations, while sometimes synthetic descriptor are preferred [8, 12]. However, there is not a one-fit-all representation and the most opportune one must be chosen, depending on the specific study aims. The calculation of the helical axis (HA) is a functional method that was proposed for studying the hinge-like joints, e.g., the knee or the elbow. In the literature, the same technique is sometimes addressed as "screw axis," "twist axis," or "axis of rotation" [13, 14]. Many authors proposed different approaches for estimating the HA and its clinical use raised a debate, concerning its validity, sensitivity to noise, and mechanical interpretation. The first studies date back to the 1980s.

This paper was meant to recap the most relevant HA calculation methods and to provide the reader with an immediate access to the calculation procedures. Some criteria for choosing the correct procedure are also discussed. The MATLAB code for the discussed procedures is provided in a repository.

✉ Andrea Ancillao
andrea.ancillao@kuleuven.be

[1] Robotics, Automation and Mechatronics (RAM) Research Group, Dept. of Mechanical Engineering, KU Leuven, box 2420, Celestijnenlaan 300, 3001 Leuven, Belgium

2 Aim

The aims of this paper are to (i) discuss the most relevant/recent literature on the HA; (ii) provide the operative equations of the most relevant calculation methods; and (iii) provide code/software for the calculation of the HA with an example.

3 Background

The HA is based on Mozzi's theorem stating that the motion of a rigid body in space can be represented as a rotation about and translation along an axis, i.e., a screw-like motion [15]. Sometimes the same theorem was attributed to the French scientist Chasles [16]. The HA was adopted in clinical motion analysis to study the human joints having a hinge-like motion, e.g., the knee [17, 18]. It was proven that the HA moves in terms of orientation and position during the motion of the joint. The variations were correlated to the functionality of the joint and to the healthiness of the ligaments [3, 7, 19, 20]. It was also suggested that the displacements of the HA were directly related to the moments exerted by muscles [21, 22] and the localization of the HA with respect to a reference can help to diagnose the loosening of the joint or prosthesis or other joint pathologies [19]. In most of the studies, the changes in orientation were reported as an angular variation, while the changes in position as the measurement of the displacement or translation of the axis. For example, in [23] the HA of the knee in subjects with injury to the cruciate ligaments was studied. The relative motion of tibia with respect to femur was measured and compared to a cohort of healthy subjects. The study demonstrated that, due to the variations in the HA, the knee is not a hinge joint, and injured knees have increased external rotation and abduction. The displacement of the HA was ~5 mm in healthy subjects and ~10 mm in injured subjects. Another study on healthy subjects calculated the HA of the knee and the instantaneous center of rotation [24]. The maximum displacement of the center of rotation was ~20 mm and the largest angular variation of the HA was ~11 deg, while another study [21] reported displacements of ~15 deg and ~30 mm.

While many studies agreed in calculating the HA of a joint based on the relative motion of the distal segment with respect to the proximal one, the reliability of such calculation was debated. In fact, the noise or the artifacts in the data may significantly affect the calculations [25, 26]. The study of [27] suggested that the minimum joint displacement required to obtain a reliable helical axis in a functional way is ~25 deg, while modern studies suggested values ~10 deg [28, 29]. Another study estimated a mean HA axis, finding that it represented a good approximation of the geometrical axis of the joint [21]. In the same study, the effect of noise on marker measurements was quantified as ~3 deg and ~8 mm respectively on angular deviation and translation of the HA.

Grip et al. [30] investigated the dynamic knee stability during squat in people with knee injuries. The analysis of the HA led to the conclusion that the injured knee was less stable than the controls. The HA variability was proven as a good indicator of knee stability. Furthermore, the variations in HA orientation were related to the rotational stability, while the translation of the HA identified the antero-posterior displacement of the joint. In a study on animal knee joints, it was observed that a pathology or damage to the ligaments led to the instability of the joint and, in turn, to changes in the direction and in the location of the HA [31]. This was also related to bone damage in the long term [31]. An increase in the variability of the HA was also observed in elderly population, where it was correlated to decreased joint stability, degeneration of the bones, and reduced neuromuscular control [29, 32]. On the contrary, athletes and young individuals tended to have less laxity and higher stability [33]. In [28], the analysis of the HA quantified the knee robustness in subjects that underwent surgery to the anterior cruciate ligaments. The operated subjects demonstrated important alterations in the knee motion strategies, although the robustness was not affected.

Another study based on models and ex vivo samples [34] proposed a signature, named "instantaneous screw parameters" for possible knee pathologies based on the HA. They considered different types of damage to the knee ligaments, each one resulting in a different helical pattern for the knee. The set of parameters included the direction and position of the HA and the variations across the motion. Such parameters were used within a trained classifier and were proved to correctly identify the different knee pathologies [34].

The design of prostheses for joint replacement is not an easy task. It must take into account several factors such as the biological compatibility, the implant stability, and the correct alignment of the rotation axes [35–37]. Thus, the HA was proved to be useful for the subject-specific design and alignment of knee prostheses, surgical guidance and loosening tests, multiscale analysis of the knee joint, and analysis of cartilage structure for applications in osteoarthritis [38]. In the work of [39], it was stressed the importance of reliably calculating an instantaneous helical axis and an average one for (i) improving the design of prostheses and (ii) evaluating the performance of the prostheses after it was implanted. The same study suggested that the variability of the instantaneous HA was correlated to the healthiness of the joint and it had to be expected as lower in healthy subjects. It was

observed that the calculation of the HA was reliable when the magnitude of angular velocity of the joint was greater than 0.25 rad/s. The same paper proposed an optimized calculation procedure for the average axis that will be discussed in the following sections.

It is known that calculating the HA via functional procedures has limitations, mainly due to measurement noise and artifacts on data. Thus, some studies recommend to rely on geometrical approaches for locating the geometrical axis of rotation [40]. For the most critical applications, where a more detailed study of the joint is required, the accurate geometry of the joint can be obtained via more invasive techniques, such as computed tomography, radiography and fluoroscopy [38, 41–43], or motion captured via markers attached to intracortical pins [21, 44, 45]. In the daily clinical practice, such as gait analysis exams, the geometrical rotation axis can be approximately located by placing markers on specific landmarks, for example, on the femur epicondyles [1, 46, 47]; however, some studies suggested that the functional approach could be more accurate and more repeatable for determining the rotation axis of hinge-like joints [27, 45, 48, 49]. The most modern measurement systems feature a relatively high signal to noise ratio and the remaining noise due to random processes be attenuated by common data processing techniques. Instead, some artifacts, such as the one due to the soft tissue displacements, are difficult to filter out and may still represent a limitation and a source of error in the calculation of the functional quantities [28, 30, 50].

4 Calculation of the helical axis

In the clinical practice, the most accurate non-invasive method to record human motion is by using the optoelectronic systems. It exploits passive markers attached to the skin of the segments composing the joint [1]. Cheaper and faster alternatives were also proposed, such as the use of inertial sensors [51, 52]. Commonly, such instruments provide the poses of the body segments expressed in the form of a homogeneous matrix [53].

Several techniques to compute the helical axis were proposed in the literature. They can be divided into two main categories: (i) techniques based on the differences in pose between two configurations (angular displacements and/or variation of the homogeneous matrix taken at two different time instants) and (ii) techniques based on the differential kinematics of the joint, mathematically represented by a screw twist, i.e., a pseudo-vector composed of the relative angular and linear velocities of the joint [54]. When the HA is computed by exploiting the relative pose of the segments composing the joint taken at any two given configurations, it is named "finite helical axis" or FHA [38, 55, 56]. Instead, when the calculation is based on the screw twist, i.e., the differential kinematics of the joint, the HA is named "instantaneous helical axis" or IHA [38, 39, 54, 57]. The concepts of the IHA and the FHA are illustrated in Fig. 1a.

When studying a motion over time (e.g., the evolution of the knee joint over a gait cycle [12]), in addition to the calculation of the IHA or FHA it is often useful to calculate an average helical axis (AHA) that conceptually represents the line that is the most parallel to the set of HAs (IHAs or FHAs) and centered to their pseudo-intersection (Fig. 1b). The AHA is usually calculated by means of an optimization procedure and in literature it is also addressed as "mean finite helical axis" [58] or "optimal flexion axis" [39]. The pseudo-intersection of the HAs is also named "optimal pivot point" [39] or "joint center" [59] or "center of rotation" [58].

In general, any axis (finite, instantaneous, or average) can be defined by a direction (unit vector) and a position (point) [13]. In the cases of IHA and FHA, the point and the direction will change over time. Additionally, previous studies proposed to define a coordinate system (CS) attached to such axes, exploiting the axis direction, position, and/or its variations [14, 57]. Such a coordinate system allowed an alternative representation of joint motion and was useful for define additional descriptive parameters for the joint [57]. The detailed calculation of such quantities is reported in the following sections.

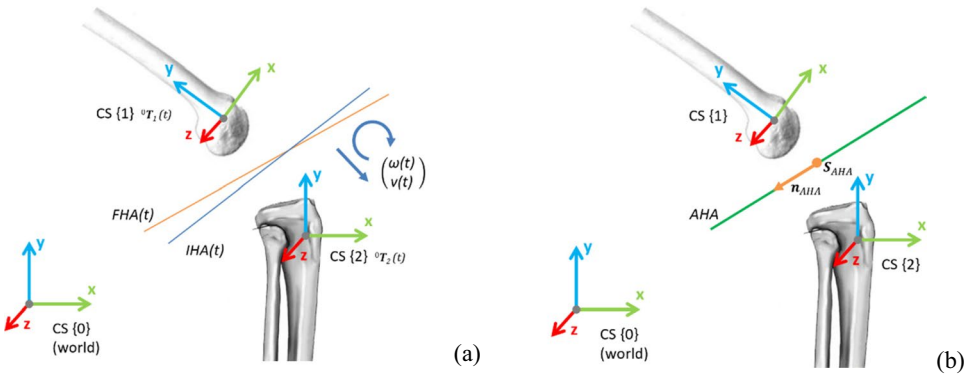

Fig. 1 Representation of **a** the instantaneous helical axis (IHA) and the finite helical axis (FHA) at a generic time *t*; **b** the average helical axis (AHA), defined by its position $\boldsymbol{S_{AHA}}$ and its direction $\boldsymbol{n_{AHA}}$

4.1 The instantaneous helical axis

The IHA is calculated based on the relative screw twist of the rigid bodies. The screw twist is a pseudo-vector composed of the angular velocity and translational velocity. It can be obtained by differentiating the homogeneous matrix representing the CS attached to a rigid body [60]. The IHA is ill-defined when the angular velocity is low; thus, many authors recommended to calculate it only when angular velocity is above a threshold. Examples of proposed values for the threshold are $\omega > 0.25$ rad/s [39] or $\omega > 0.1\omega_{max}$ [61]. The IHA can be calculated according to the following procedure ([39, 57]).

To represent the motion of a joint, we consider (i) the pose of the proximal segment {1}, with respect to the lab. CS {0}, represented as ${}^{0}\boldsymbol{T}_1$, and (ii) the pose of the distal segment {2}, ${}^{0}\boldsymbol{T}_2$. We then calculate the differential kinematics (screw twist), ${}^{\mathbf{0}}\boldsymbol{t_k}$, associated to the k-th pose, with respect to the CS {0}. Naming ${}^{0}\boldsymbol{O}_k$ the origin of the k-th pose seen in the CS {0}, and ${}^{0}\boldsymbol{q}_k$ the quaternion representation of the orientation ${}^{0}\boldsymbol{R}_k$ associated to the k-th CS, we have [60]:

$$ {}^{\mathbf{0}}\boldsymbol{\omega_k} = 2\mathrm{E}\,{}^{0}\dot{\boldsymbol{q}}_k \tag{1} $$

$$ {}^{\mathbf{0}}\boldsymbol{\omega_k} = 2\begin{pmatrix} -q_1 & q_0 & -q_3 & q_2 \\ -q_2 & q_3 & q_0 & -q_1 \\ -q_3 & -q_2 & q_1 & q_0 \end{pmatrix}\begin{pmatrix} {}^{0}\dot{q}_{k,0} \\ {}^{0}\dot{q}_{k,1} \\ {}^{0}\dot{q}_{k,2} \\ {}^{0}\dot{q}_{k,3} \end{pmatrix} \tag{2} $$

$$ {}^{\mathbf{0}}\boldsymbol{v_k} = \left({}^{\mathbf{0}}\boldsymbol{O_k} \times {}^{\mathbf{0}}\boldsymbol{\omega_k}\right) + {}^{0}\dot{\boldsymbol{O}}_k \tag{3} $$

$$ {}^{\mathbf{0}}\boldsymbol{t_k} = \left({}^{\mathbf{0}}\boldsymbol{\omega_k}, {}^{\mathbf{0}}\boldsymbol{v_k}\right) \tag{4} $$

We then calculate the relative screw twist of the joint and transform it to a local CS, for example, of segment 1:

$$ {}^{\mathbf{0}}\boldsymbol{t_{2-1}} = {}^{\mathbf{0}}\boldsymbol{t_2} - {}^{\mathbf{0}}\boldsymbol{t_1} \tag{5} $$

$$ {}^{\mathbf{1}}\boldsymbol{t_{2-1}} = {}^{\mathbf{1}}\boldsymbol{U_0}\,{}^{\mathbf{0}}\boldsymbol{t_{2-1}} \tag{6} $$

where ${}^{\mathbf{1}}\boldsymbol{U_0}$ is the screw transformation matrix from {0} to {1} based on the orientation ${}^{1}\boldsymbol{R}_0$:

$$ {}^{\mathbf{1}}\boldsymbol{U_0} = \begin{pmatrix} \ddots & \vdots & \iddots & 0 & 0 & 0 \\ \cdots & {}^{\mathbf{1}}\boldsymbol{R_0} & \cdots & 0 & 0 & 0 \\ \iddots & \vdots & \ddots & 0 & 0 & 0 \\ \ddots & \vdots & \iddots & \ddots & \vdots & \iddots \\ \cdots & {}^{\mathbf{1}}\boldsymbol{O_0}\ {}^{\mathbf{1}}\boldsymbol{R_0} & \cdots & \cdots & {}^{\mathbf{1}}\boldsymbol{R_0} & \cdots \\ \iddots & \vdots & \ddots & \iddots & \vdots & \ddots \end{pmatrix} \tag{7} $$

Having the screw twist of body {2} with respect to {1} expressed in {1} (Eq. 6), we can immediately calculate the direction ${}^{1}\boldsymbol{n_{IHA}}$ and position ${}^{1}\boldsymbol{S_{IHA}}$ of the IHA, expressed in CS {1} [39]:

$$ {}^{1}\boldsymbol{n_{IHA}} = \pm\frac{{}^{\mathbf{1}}\boldsymbol{\omega_{2-1}}}{\left\|{}^{\mathbf{1}}\boldsymbol{\omega_{2-1}}\right\|} \tag{8} $$

$$ {}^{1}\boldsymbol{S_{IHA}} = \frac{{}^{\mathbf{1}}\boldsymbol{\omega_{2-1}} \times {}^{\mathbf{1}}\boldsymbol{v_{2-1}}}{\left\|{}^{\mathbf{1}}\boldsymbol{\omega_{2-1}}\right\|^2} \tag{9} $$

Note that the IHA takes the direction from the angular velocity. If a specific direction is needed, the sign in Eq. 8 must be opportunely chosen. ${}^{1}\boldsymbol{n_{IHA}}$ and ${}^{1}\boldsymbol{S_{IHA}}$ are time-dependent quantities; in Eq. 8 and 9, the time dependency was omitted to simplify the notation.

4.2 The finite helical axis

The finite helical axis (FHA), also known as finite screw axis, is calculated based on poses at two different time-steps [55, 56]. It differs from the IHA as the FHA does not require the calculation of the screw twist, but it is based on the finite changes in the pose: considering the motion of a joint, we name the pose of the proximal segment with respect to the lab CS as ${}^{0}\boldsymbol{T}_1$, and the one of the distal segment as ${}^{0}\boldsymbol{T}_2$. We can calculate the relative pose and consider its finite variation between two different time-samples, namely, i_1 and i_2.

$$ {}^{1}\boldsymbol{T}_2 = \left({}^{0}\boldsymbol{T}_1\right)^{-1}{}^{0}\boldsymbol{T}_2 \tag{10} $$

$$ {}^{1}\boldsymbol{T}_{i1\to i2} = \left({}^{1}\boldsymbol{T_2}(i_1)\right)\left({}^{1}\boldsymbol{T_2}(i_2)\right)^{-1} \tag{11} $$

that can be decomposed in the rotation and translation parts: ${}^{\mathbf{1}}\boldsymbol{R}$ and ${}^{\mathbf{1}}\boldsymbol{O}$.

Naming $R_{x,y}$ the elements of the ${}^{\mathbf{1}}\boldsymbol{R}$ matrix, we have [56]:

$$ \sin(\varphi) = \frac{1}{2}\sqrt{\left(R_{3,2} - R_{2,3}\right)^2 + \left(R_{1,3} - R_{3,1}\right)^2 + \left(R_{2,1} - R_{1,2}\right)^2} \tag{12} $$

$$ \cos(\varphi) = \frac{1}{2}\left(R_{1,1} + R_{2,2} + R_{3,3} - 1\right) \tag{13} $$

$$ \varphi = \begin{cases} \arcsin(\sin(\varphi)) \mid \sin(\varphi) \le \frac{\sqrt{2}}{2} \\ \arccos(\cos(\varphi)) \mid \sin(\varphi) > \frac{\sqrt{2}}{2} \end{cases} \tag{14} $$

$$ {}^{1}\boldsymbol{n_{FHA}} = \frac{1}{2\sin(\varphi)}\begin{bmatrix} R_{3,2} - R_{2,3} \\ R_{1,3} - R_{3,1} \\ R_{2,1} - R_{1,2} \end{bmatrix}^T \tag{15} $$

$$d = {}^{1}\boldsymbol{n}_{FHA}{}^{T} \bullet {}^{1}\boldsymbol{O} \tag{16}$$

$${}^{1}\boldsymbol{S}_{FHA} = -\frac{1}{2}{}^{1}\boldsymbol{n}_{FHA} \times \left({}^{1}\boldsymbol{n}_{FHA} \times {}^{1}\boldsymbol{O}\right) + \frac{\sin(\varphi)}{2(1-\cos(\varphi))}\left({}^{1}\boldsymbol{n}_{FHA} \times {}^{1}\boldsymbol{O}\right) \tag{17}$$

where φ and d are the angle of rotation about and the displacement along the FHA.

4.3 Coordinate system associated to the helical axis

For several practical purposes, it is useful to define a CS attached to the helical axis [62]. Such a CS is functionally-defined, meaning that it does not require the knowledge of specific anatomical landmarks, but it can carry useful information about the motion. For example, clinically relevant alterations in joint displacement can be expressed with respect to this CS [62]. It can be defined with respect to any CS according to the following equations [57]. The CS evolves with the motion, in other words, it is time-dependent (the time-dependency was not indicated in the following equations to simplify the notation).

The HA frame is then represented by a (4×4) homogeneous matrix.

- Origin: $\boldsymbol{S}_{\mathbf{HA}}$;
- $\hat{\boldsymbol{e}}_3$: the HA direction $\boldsymbol{n}_{\mathbf{HA}}$;
- $\hat{\boldsymbol{e}}_2 = \frac{\boldsymbol{n}_{\mathbf{HA}} \times \boldsymbol{S}_{\mathbf{HA}}}{\|\boldsymbol{n}_{\mathbf{HA}} \times \boldsymbol{S}_{\mathbf{HA}}\|}$ (18)
- $\hat{\boldsymbol{e}}_1 = \hat{\boldsymbol{e}}_3 \times \hat{\boldsymbol{e}}_2$

$$\boldsymbol{T}_{HA} = \begin{bmatrix} \vdots & \vdots & \vdots & \vdots \\ \hat{\boldsymbol{e}}_1 & \hat{\boldsymbol{e}}_2 & \hat{\boldsymbol{e}}_3 & \boldsymbol{S}_{HA} \\ \vdots & \vdots & \vdots & \vdots \\ 0 & 0 & 0 & 1 \end{bmatrix} \tag{19}$$

Alternatively, the second axis of the CS can be defined in a slightly different way, when information about the angular velocity of CS {2} with respect to CS {1}, $\boldsymbol{\omega}_{\mathbf{2,1}}$, is available [57]:

$$\hat{\boldsymbol{e}}_2 = \frac{\boldsymbol{\omega}_{\mathbf{2,1}} \times \dot{\boldsymbol{\omega}}_{\mathbf{2,1}}}{\left\|\boldsymbol{\omega}_{\mathbf{2,1}} \times \dot{\boldsymbol{\omega}}_{\mathbf{2,1}}\right\|} \tag{20}$$

It is also possible to define a local coordinate system associated to the AHA. The procedure is the same illustrated in Eqs. (18) and (19). The coordinate system associated to the AHA is not time-dependent.

4.4 The average helical axis and the center of rotation

The calculation of an average helical axis is usually achieved via optimization procedures designed to accurately locate (i) the AHA direction (unit vector, $\boldsymbol{n}_{\boldsymbol{AHA}}$) that is "the most parallel" to the set of helical axes and (ii) the position of the AHA (point $\boldsymbol{S}_{\boldsymbol{AHA}}$), i.e., the pseudo-intersection of the IHAs, also known as "optimal pivot point" or "center of rotation" and it is defined as the point that has the minimum root mean square distance from a set of N HAs [59]. The AHA is not time-dependent like the IHA and the FHA. The AHA is expressed in the same CS as the IHA or FHA, for example, {1}.

The simplest way for calculating the position of the AHA is by solving a least squares problem [39]:

$$\boldsymbol{S}_{\boldsymbol{AHA}} = \left(\frac{1}{N}\sum_{i=1}^{N} w_i\left(\boldsymbol{I} - \boldsymbol{n}_i\boldsymbol{n}_i^{T}\right)\right)^{-1}\left(\frac{1}{N}\sum_{i=1}^{N} w_i\left(\boldsymbol{I} - \boldsymbol{n}_i\boldsymbol{n}_i^{T}\right)\boldsymbol{S}_i\right) \tag{21}$$

where $\boldsymbol{n}_i$ and $\boldsymbol{S}_i$ are respectively the direction of the i-th helical axis, seen in CS {1}; N is the total number of axes in the set; and w_i is a weight factor.

The direction of the AHA, $\boldsymbol{n}_{\boldsymbol{AHA}}$, i.e., the unit vector "most parallel" to the set of ISAs, can be obtained as the eigenvector associated to the largest eigenvalue of the following expression [59]:

$$\sum_{i=1}^{N} w_i\left(\boldsymbol{n}_i\boldsymbol{n}_i^{T}\right) \tag{22}$$

As the HA is ill-defined for low angular velocities or small angular displacements, some previous studies recommended to exclude from the computing the samples where the magnitude of the angular velocity is below the chosen threshold [39], see "Section 4.1." An alternative way to deal with ill-defined HAs is to introduce a weighting factor based on the instantaneous angle or angular velocity [59]. Two possible definitions for the i-th weight that were proposed are the following:

$$w_i = \sin^2\left(\frac{\varphi_i}{2}\right) \tag{23}$$

or:

$$w_i = f\left(\frac{\|\boldsymbol{\omega}_i\|}{\max_t\|\boldsymbol{\omega}\|}\right) \tag{24}$$

$$f(x) = \frac{L}{1 + e^{-k(x-x0)}} \tag{25}$$

where $f(x)$ is the logistic function with parameters L, k, and $x0$. A typical choice of the parameters is $L = 1$, $x0 = 0{,}5$, and $k = 20$.

A different approach to calculate the AHA exploits the measured orientation of the joint taken at an i-th and a j-th time instants, with $i \neq j$. All the possible combinations $\boldsymbol{R}_i\boldsymbol{R}_j$ are considered, as well as the respective screw points $\boldsymbol{s}_{i,j}$ occurring during the motion [59].

$$\boldsymbol{n}_{AHA} = \arg\min_{\boldsymbol{n}\in R^3} \boldsymbol{n}^T \left(N(N-1)\boldsymbol{I}_3 - \sum_{i,j=1,i\neq j}^{N} \boldsymbol{R}_i\boldsymbol{R}_j^T \right)\boldsymbol{n} \tag{26}$$

$$\boldsymbol{s}_A = \arg\min_{\boldsymbol{s}\in R^3} \sum_{i,j=1,i<j}^{N} w_{i,j}\left\{ (\boldsymbol{s}-\boldsymbol{s}_{i,j}) - \left[(\boldsymbol{s}-\boldsymbol{s}_{i,j})^T \boldsymbol{n}_{i,j} \right]\boldsymbol{n}_{i,j} \right\}^2 \tag{27}$$

that can be minimized by means of a least squares approach. In this case, the weighting factor is defined based on the angle between the i-th and j-th instants:

$$w_{i,j} = \sin^2\left(\frac{\varphi_{i,j}}{2}\right) \tag{28}$$

This approach takes into account all the possible (i,j) combinations across the N samples; thus, it is computationally slower than the other methods. However, it was suggested that this approach may be less sensitive to noise [63]. When AHA is calculated according to this approach, it is sometimes named "mean finite helical axis" MFHA [59].

4.5 Dispersion analysis

When the helical axis is used to characterize the behavior of a human joint or a hinge-like joint, it is useful to quantify its deviation and dispersion from a reference [24]. The reference can be geometrically defined (e.g., the condyle to condyle line in the knee [64, 65] or the rotation axis of a prosthesis [43]) or functionally defined (e.g., the AHA previously described). Some studies also suggested to use anatomical planes as a reference [21, 29, 62, 65, 66]. A typical way to quantify the deviation from the reference is by calculating (i) the instantaneous angle and (ii) the instantaneous distance between the HA and the reference. The angle can be obtained via the dot product of the unit direction vectors of the HA and the reference:

$$\vartheta_i = \cos^{-1}\left(\boldsymbol{n}_i \bullet \boldsymbol{n}_{AHA}\right) \tag{29}$$

while the distance can be obtained via the Euclidean distance between $\boldsymbol{S}_i$ and $\boldsymbol{S}_{AHA}$.

The root mean square error in the calculation of the AHA, i.e., the quantification of the dispersion of the IHA with respect to the AHA, in terms of position error and direction error can be estimated as [39]

$$E_S = \sqrt{\frac{1}{N}\sum_{i=1}^{N} \left|\boldsymbol{S}_{AHA} - \boldsymbol{s}_i\right|^2} \tag{30}$$

$$E_{\boldsymbol{n}} = \sqrt{\frac{1}{N}\sum_{i=1}^{N} \vartheta_i^{\,2}} \tag{31}$$

Another method to quantify the dispersion in the deviation of the IHA with respect to the reference is to define a plane and calculate the intersection of the IHA with this plane [21, 62, 67]. Commonly, the plane is defined as perpendicular to the reference axis and at a unit distance from the CoR. The intersection points can be visualized as a cloud of points on the plane and the dispersion can be quantified via the dimensions of the confidence ellipse, i.e., the ellipse that contains the 95% of the points. The axes of the ellipse are calculated via a principal component analysis procedure [54].

4.6 Example

An example of calculation is illustrated in detail within the code in the supplementary material.

The example considers the recorded motion of a mechanical hinge joint left free to swing after an initial perturbation. The motion was recorded by means of an optoelectronic system and passive markers. The motion was represented by means of the pose of the distal segment, CS {2} with respect to the proximal one, CS {1}. The differential kinematics were obtained as the derivative of the poses (Figs. 2, 3, 4, and 5). Then all the previously described quantities were computed (Table 1).

5 Discussion

This paper presented a review of the operative equations for calculating the IHA, FHA, AHA, a coordinate system attached to the helical axes, and finally, some parameters for the quantitative analysis of the dispersion of the IHA/FHA with respect to a reference.

The IHA and FHA are different computational approaches, although the clinical interpretation of the resulting axes was proven to be equivalent [59]. Both approaches allow the functional analysis of joints via the calculation of (i) the center of rotation (CoR), that can be defined as the pseudo-intersection of the set of the helical axes and (ii) the average helical axis, that is the average direction among the set of helical axes [39, 59].

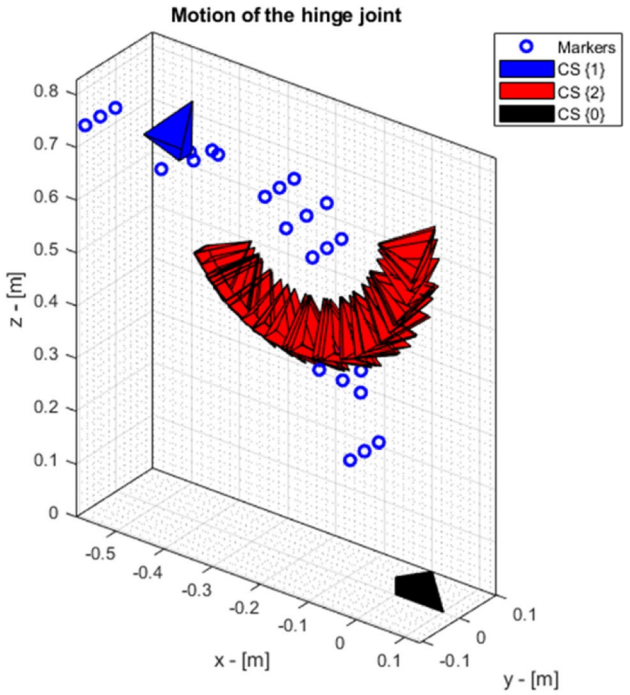

Fig. 2 Recorded motion data for the hinge joint. The motion is represented by the coordinate systems (CS) of the segments {1} and {2} with respect to the lab {0}

Knowledge of the CoR is useful for sphere-like joints, such as the hip or the shoulder, while the AHA is often used to represent the axis of rotation in hinge-like joints. It finds applications in the design of prostheses, their placement, and post-operatory testing [8, 37, 39].

The choice of the computational approach should be based on the features of the data available. The IHA requires knowing the differential kinematics; thus, it should be privileged when the direct measurement of velocities is available, e.g., when inertial sensors or dedicated sensors are used [14]. Differential kinematics can also be obtained from pose measurements, but it will require the computing of derivatives. This means that it is still possible to calculate the IHA from pose measurements, but the noise on the data represents a limitation, as it will be amplified by the numerical procedures. Such phenomenon can be mitigated by means of filters and noise reduction techniques, and high sampling frequencies have to be preferred [1, 68, 69]. The FHA approach, instead, does not require high sampling frequencies nor the calculation of derivatives, as it is based on the measured orientation of the joint segments and their position. The drawback of this approach is that it is computationally demanding. Very high sampling frequencies may lead to longer processing times, making it unsuitable for real-time applications.

The main source of error for both methods is the presence of noise and artifacts affecting the data. In particular, the soft tissue artifact [50, 70] may induce an error in the measurement of the position and the orientation of joint segments that, in turn, leads to a wrong position and orientation of the HA or AHA. This effect must be considered when studying the motion of biological apparatus, such as the human body.

From a clinical point of view, the dispersion analysis is the tool that allows the quantitative evaluation of the joint displacement. An example is the knee joint, that it is known to have a physiological range of variation of the HA that can be extended or reduced in case of pathologies to

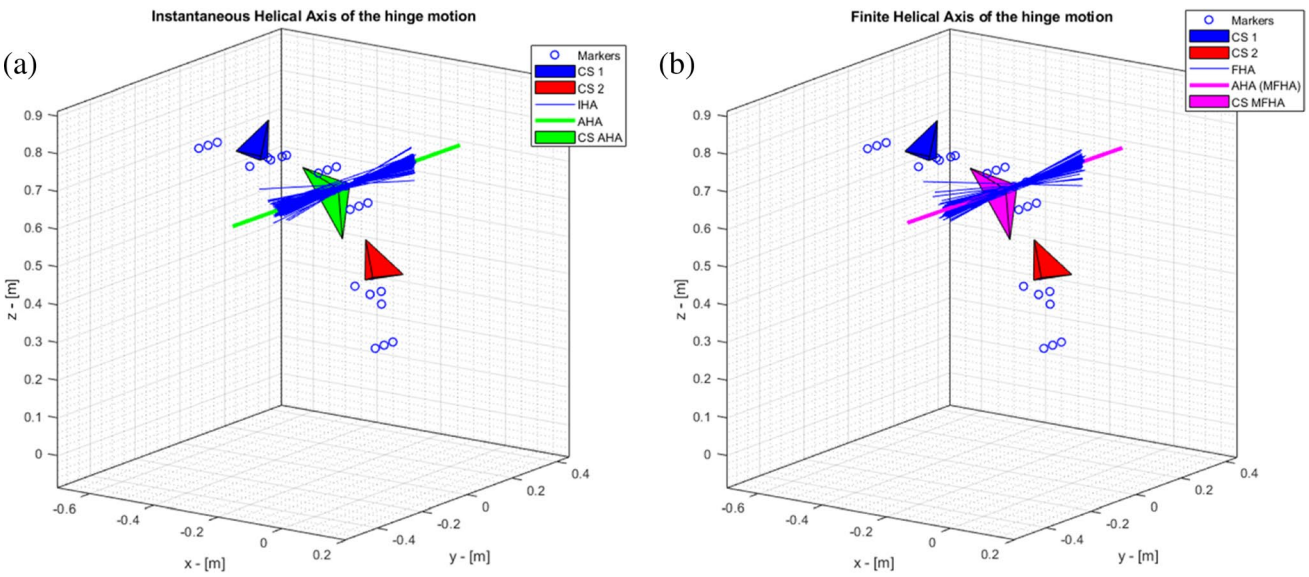

Fig. 3 Calculation and visualization of the previously described quantities: **a** instantaneous helical axis, **b** finite helical axis

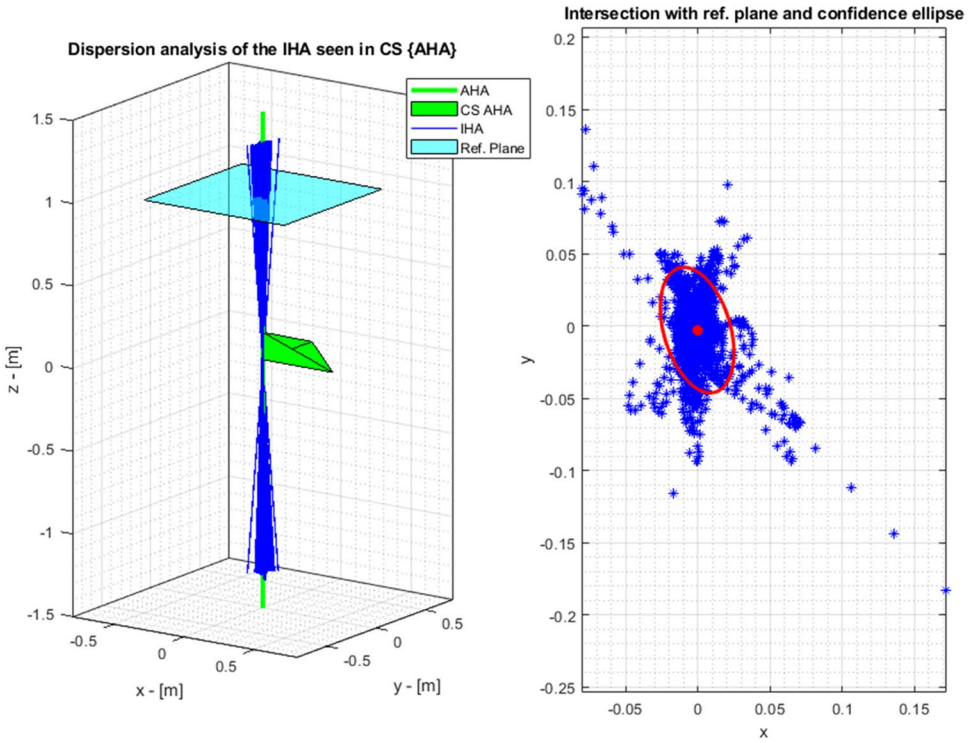

Fig. 4 Dispersion analysis of the instantaneous helical axis

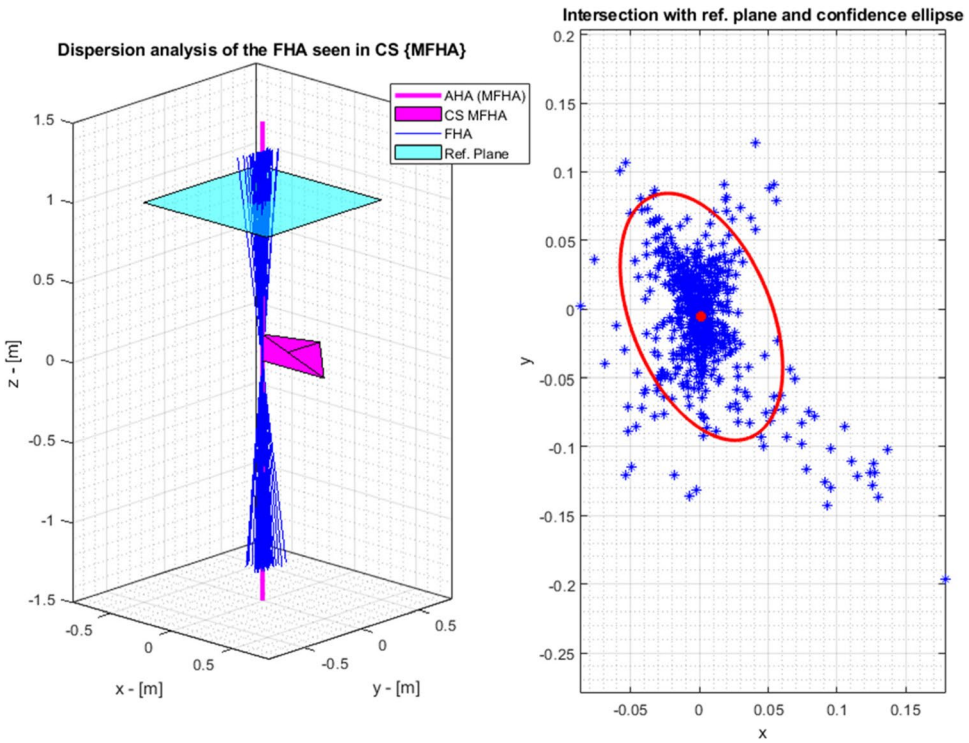

Fig. 5 Dispersion analysis of the finite helical axis

Table 1 Results of the dispersion analysis on the example data

	IHA	FHA
E_S [mm]	1.5	2.0
E_n [deg.]	1.8	2.8

the ligaments [2, 7, 31, 67]. In these cases, the dispersion parameters previously discussed provide the quantitative analysis of the deviation from a "perfect hinge" ideal case.

6 Conclusion

This paper discussed the calculation of the instantaneous helical axis, the finite helical axis, and the average screw axis. Such quantities were proven useful in the clinical practice as they provided (i) information on the healthiness of a joint or a prosthesis and (ii) a functional way for estimating the axis or the center of rotation of the joint. Although the calculation procedure is different, the IHA and the AHA have an equivalent meaning and anatomical interpretation. The IHA is based on differential kinematics, i.e., the velocity of the joint, while the FHA is based on the finite angular displacement and measured poses of the segments. The choice of the method should depend on the features of the available data, such as the type of data, the signal to noise ratio, and the sampling frequency. When differential kinematics are available as direct measurements, and/or the signal to noise ratio is high, the IHA may be the preferred choice. When pose measurements are available, and in the cases where the sampling frequency is low, the FHA may be the better choice as it can be effectively adopted when a more discrete description of the joint motion is required. The AHA, being a constant axis, is a good estimator for the rotation axis of hinge-like joints. The calculation of the AHA based on all the possible pairs of FHA is computationally slower but more resistant to noise.

Code availability The code provided was designed to sequentially calculate the IHA, the FHA, the AHA, and the respective parameters and dispersion analysis. All the quantities were calculated on a sample dataset containing the measurements of an artificial hinge joint.

The MATLAB code can be accessed through the following GitHub repository: https://github.com/Andrea14-ing/IHA_paper.

Please run the example included in the "MAIN.m" script. Further instructions are provided within the file.

Declarations

Conflict of interest The author declares no competing interests.

References

1. Ancillao A (2018) Stereophotogrammetry in functional evaluation: history and modern protocols. In: SpringerBriefs in applied sciences and technology. pp 1–29
2. Ancillao A, Rossi S, Cappa P (2017) Analysis of knee strength measurements performed by a hand-held multicomponent dynamometer and optoelectronic system. IEEE Trans Instrum Meas 66:85–92. https://doi.org/10.1109/TIM.2016.2620799
3. Ancillao A (2019) An experimental analysis of the sources of inaccuracy occurring in hip strength measurements conducted by hand held dynamometry. Eur J Phys 0:1–6. https://doi.org/10.1080/21679169.2019.1646802
4. Ancillao A, Savastano B, Galli M, Albertini G (2017) Three dimensional motion capture applied to violin playing: a study on feasibility and characterization of the motor strategy. Comput Methods Prog Biomed 149:19–27. https://doi.org/10.1016/j.cmpb.2017.07.005
5. Ancillao A (2018) A new method for the quality assurance of strength measurements. In: SpringerBriefs in applied sciences and technology. pp 31–88
6. Rutz E, Baker R, Tirosh O et al (2011) Tibialis anterior tendon shortening in combination with Achilles tendon lengthening in spastic equinus in cerebral palsy. Gait Posture 33:152–157. https://doi.org/10.1016/j.gaitpost.2010.11.002
7. Brunner R, Rutz E (2013) Biomechanics and muscle function during gait. J Child Orthop 7:367–371. https://doi.org/10.1007/s11832-013-0508-5
8. Ozada N, Ghafoorpoor Yazdi S, Khandan A, Karimzadeh M (2017) A brief review of reverse shoulder prosthesis: arthroplasty, complications, revisions, and development. Trauma Mon 23. https://doi.org/10.5812/traumamon.58163
9. Ancillao A (2019) An experimental analysis of the sources of inaccuracy occurring in hip strength measurements conducted by hand held dynamometry. Eur J Phys. https://doi.org/10.1080/21679169.2019.1646802
10. Steinwender G, Saraph V, Scheiber S et al (2000) Intrasubject repeatability of gait analysis data in normal and spastic children. Clin Biomech 15:134–139. https://doi.org/10.1016/S0268-0033(99)00057-1
11. Vismara L, Cimolin V, Galli M, et al (2016) Osteopathic manipulative treatment improves gait pattern and posture in adult patients with Prader–Willi syndrome. Int J Osteopath Med 19:35–43. https://doi.org/10.1016/j.ijosm.2015.09.001
12. Ancillao A, van der Krogt MM, Buizer AI et al (2017) Analysis of gait patterns pre- and post-single event multilevel surgery in children with cerebral palsy by means of offset-wise movement analysis profile and linear fit method. Hum Mov Sci 55:145–155. https://doi.org/10.1016/j.humov.2017.08.005
13. Woltring HJ, Huiskes R, de Lange A, Veldpaus FE (1985) Finite centroid and helical axis estimation from noisy landmark measurements in the study of human joint kinematics. J Biomech 18:379–389. https://doi.org/10.1016/0021-9290(85)90293-3
14. Ancillao A, Vochten M, Aertbeliën E et al (2020) Estimating the instantaneous screw axis and the screw axis invariant descriptor of motion by means of inertial sensors: an experimental study with a mechanical hinge joint and comparison to the optoelectronic system. Sensors (Switzerland) 20. https://doi.org/10.3390/s20010049
15. Mozzi G (1763) Discorso matematico sopra il rotamento momentaneo dei corpi. Stamperia del Donato Campo, Napoli
16. Chasles M (1830) Note sur les propriétés génerales du système de deux corps semblables entr'eux et placés d'une manière quelconque dans l'espace; et sur le déplacement fini ou infiniment petit d'un corps solide libre [A note on the general properties of a system of two si. Bull des Sci Mathématiques, Férussac 14:321–326
17. Martelli S (2003) New method for simultaneous anatomical and functional studies of articular joints and its application to the human knee. Comput Methods Prog Biomed 70:223–240. https://doi.org/10.1016/S0169-2607(02)00028-7
18. Martelli S, Zaffagnini S, Falcioni B, Marcacci M (2000) Intraoperative kinematic protocol for knee joint evaluation. Comput Methods Prog Biomed 62:77–86. https://doi.org/10.1016/S0169-2607(99)00055-3
19. Sheehan FT (2010) The instantaneous helical axis of the subtalar and talocrural joints: a non-invasive in vivo dynamic study. J Foot Ankle Res 3:13. https://doi.org/10.1186/1757-1146-3-13
20. Ancillao A (2018) Modern functional evaluation methods for muscle strength and gait analysis. Springer International Publishing, International

21. van den Bogert AJ, Reinschmidt C, Lundberg A (2008) Helical axes of skeletal knee joint motion during running. J Biomech 41:1632–1638. https://doi.org/10.1016/j.jbiomech.2008.03.018
22. Geier A, Aschemann H, D'Lima D et al (2018) Force closure mechanism modeling for musculoskeletal multibody simulation. IEEE Trans Biomed Eng 65:2471–2482. https://doi.org/10.1109/TBME.2018.2800293
23. Shiavi R, Limbird T, Frazer M et al (1987) Helical motion analysis of the knee—II. Kinematics of uninjured and injured knees during walking and pivoting. J Biomech 20:653–665. https://doi.org/10.1016/0021-9290(87)90032-7
24. Hart RA, Mote CD, Skinner HB (1991) A finite helical axis as a landmark for kinematic reference of the knee. J Biomech Eng 113:215–222. https://doi.org/10.1115/1.2891237
25. Frigo C, Rabuffetti M (1998) Multifactorial estimation of hip and knee joint centres for clinical application of gait analysis. Gait Posture 8:91–102. https://doi.org/10.1016/S0966-6362(98)00031-9
26. Leardini A, Chiari L, Della CU, Cappozzo A (2005) Human movement analysis using stereophotogrammetry: part 3. Soft tissue artifact assessment and compensation. Gait Posture 21:212–225. https://doi.org/10.1016/j.gaitpost.2004.05.002
27. Chèze L, Fregly BJ, Dimnet J (1998) Determination of joint functional axes from noisy marker data using the finite helical axis. Hum Mov Sci 17:1–15. https://doi.org/10.1016/S0167-9457(97)00018-3
28. Markström JL, Grip H, Schelin L, Häger CK (2020) Individuals with an anterior cruciate ligament–reconstructed knee display atypical whole body movement strategies but normal knee robustness during side-hop landings: a finite helical axis analysis. Am J Sports Med 48:1117–1126. https://doi.org/10.1177/0363546520910428
29. Temporiti F, Cescon C, Adamo P et al (2020) Dispersion of knee helical axes during walking in young and elderly healthy subjects. J Biomech 109:109944. https://doi.org/10.1016/j.jbiomech.2020.109944
30. Grip H, Tengman E, Häger CK (2015) Dynamic knee stability estimated by finite helical axis methods during functional performance approximately twenty years after anterior cruciate ligament injury. J Biomech 48:1906–1914. https://doi.org/10.1016/j.jbiomech.2015.04.016
31. Barton KI, Shekarforoush M, Heard BJ et al (2019) Three-dimensional in vivo kinematics and finite helical axis variables of the ovine stifle joint following partial anterior cruciate ligament transection. J Biomech 88:78–87. https://doi.org/10.1016/j.jbiomech.2019.03.021
32. Rosenbaum D (2009) Human motor control, 2nd edn. Academic Press
33. Markström JL, Grip H, Schelin L, Häger CK (2019) Dynamic knee control and movement strategies in athletes and non-athletes in side hops: implications for knee injury. Scand J Med Sci Sports 29:sms.13432. https://doi.org/10.1111/sms.13432
34. Wolf A, Degani A (2007) Recognizing knee pathologies by classifying instantaneous screws of the six degrees-of-freedom knee motion. Med Biol Eng Comput 45:475–482. https://doi.org/10.1007/s11517-007-0174-1
35. Qin W, Kolooshani A, Kolahdooz A et al (2021) Coating the magnesium implants with reinforced nanocomposite nanoparticles for use in orthopedic applications. Colloids Surfaces A Physicochem Eng Asp 621:126581. https://doi.org/10.1016/j.colsurfa.2021.126581
36. Esmaeili S, Akbari Aghdam H, Motififard M et al (2020) A porous polymeric–hydroxyapatite scaffold used for femur fractures treatment: fabrication, analysis, and simulation. Eur J Orthop Surg Traumatol 30:123–131. https://doi.org/10.1007/s00590-019-02530-3
37. Bagherifard A, Joneidi Yekta H, Akbari Aghdam H et al (2020) Improvement in osseointegration of tricalcium phosphate-zircon for orthopedic applications: an in vitro and in vivo evaluation. Med Biol Eng Comput 58:1681–1693. https://doi.org/10.1007/s11517-020-02157-1
38. Millán Vaquero RM, Vais A, Dean Lynch S et al (2016) Helical axis data visualization and analysis of the knee joint articulation. J Biomech Eng 138. https://doi.org/10.1115/1.4034005
39. Stokdijk M, Meskers CGM, Veeger HEJ et al (1999) Determination of the optimal elbow axis for evaluation of placement of prostheses. Clin Biomech 14:177–184. https://doi.org/10.1016/S0268-0033(98)00057-6
40. Schwartz MH, Rozumalski A (2005) A new method for estimating joint parameters from motion data. J Biomech 38:107–116. https://doi.org/10.1016/j.jbiomech.2004.03.009
41. Barre A, Thiran J-P, Jolles BM et al (2013) Soft tissue artifact assessment during treadmill walking in subjects with total knee arthroplasty. IEEE Trans Biomed Eng 60:3131–3140. https://doi.org/10.1109/TBME.2013.2268938
42. Zumbrunn T, Schütz P, von Knoch F et al (2019) Medial unicompartmental knee arthroplasty in ACL-deficient knees is a viable treatment option: in vivo kinematic evaluation using a moving fluoroscope. Knee Surgery, Sport Traumatol Arthrosc. https://doi.org/10.1007/s00167-019-05594-0
43. Akbari Shandiz M, Boulos P, Saevarsson SK et al (2016) Changes in knee kinematics following total knee arthroplasty. Proc Inst Mech Eng Part H J Eng Med 230:265–278. https://doi.org/10.1177/0954411916632491
44. Reinschmidt C, van den Bogert A, Lundberg A et al (1997) Tibiofemoral and tibiocalcaneal motion during walking: external vs. skeletal markers. Gait Posture 6:98–109. https://doi.org/10.1016/S0966-6362(97)01110-7
45. Ramsey DK, Wretenberg PF (1999) Biomechanics of the knee: methodological considerations in the in vivo kinematic analysis of the tibiofemoral and patellofemoral joint. Clin Biomech 14:595–611. https://doi.org/10.1016/S0268-0033(99)00015-7
46. Davis RB, Ounpuu S, Gage JR (1991) A gait analysis data collection and reduction technique. Hum Mov Sci 10:575–587
47. Ferrari A, Benedetti MG, Pavan E et al (2008) Quantitative comparison of five current protocols in gait analysis. Gait Posture 28:207–216. https://doi.org/10.1016/j.gaitpost.2007.11.009
48. Besier TF, Sturnieks DL, Alderson JA, Lloyd DG (2003) Repeatability of gait data using a functional hip joint centre and a mean helical knee axis. J Biomech 36:1159–1168. https://doi.org/10.1016/S0021-9290(03)00087-3
49. Temporiti F, Furone R, Cescon C et al (2019) Dispersion of helical axes during shoulder movements in young and elderly subjects. J Biomech 88:72–77. https://doi.org/10.1016/j.jbiomech.2019.03.018
50. Ancillao A, Aertbeliën E, De Schutter J (2021) Effect of the soft tissue artifact on marker measurements and on the calculation of the helical axis of the knee during a gait cycle: a study on the CAMS-Knee data set. Hum Mov Sci 80:102866. https://doi.org/10.1016/j.humov.2021.102866
51. Rueterbories J, Spaich EG, Larsen B, Andersen OK (2010) Methods for gait event detection and analysis in ambulatory systems. Med Eng Phys 32:545–552. https://doi.org/10.1016/j.medengphy.2010.03.007
52. Ancillao A, Tedesco S, Barton J, O'Flynn B (2018) Indirect measurement of ground reaction forces and moments by means of wearable inertial sensors: a systematic review. Sensors 18:2564. https://doi.org/10.3390/s18082564
53. Cappozzo A, Della Croce U, Leardini A, Chiari L (2005) Human movement analysis using stereophotogrammetry part 1: theoretical background. Gait Posture 21:186–196. https://doi.org/10.1016/j.gaitpost.2004.01.010

54. Ancillao A, Vochten M, Aertbeliën E et al (2019) Estimating the instantaneous screw axis and the screw axis invariant descriptor of motion by means of inertial sensors: an experimental study with a mechanical hinge joint and comparison to the optoelectronic system. Sensors 20:49. https://doi.org/10.3390/s20010049
55. Spoor CW, Veldpaus FE (1980) Rigid body motion calculated from spatial co-ordinates of markers. J Biomech 13:391–393. https://doi.org/10.1016/0021-9290(80)90020-2
56. Shekarforoush M, Beveridge JE, Hart DA et al (2018) Correlation between translational and rotational kinematic abnormalities and osteoarthritis-like damage in two in vivo sheep injury models. J Biomech 75:67–76. https://doi.org/10.1016/j.jbiomech.2018.04.046
57. De Schutter J (2010) Invariant description of rigid body motion trajectories. J Mech Robot 2:011004. https://doi.org/10.1115/1.4000524
58. Ehrig RM, Heller MO, Kratzenstein S et al (2011) The SCoRE residual: a quality index to assess the accuracy of joint estimations. J Biomech 44:1400–1404. https://doi.org/10.1016/j.jbiomech.2010.12.009
59. Ehrig RM, Heller MO (2019) On intrinsic equivalences of the finite helical axis, the instantaneous helical axis, and the SARA approach. A mathematical perspective. J Biomech 84:4–10. https://doi.org/10.1016/j.jbiomech.2018.12.034
60. Graf B (2008) Quaternions and dynamics. arXiv 2008:
61. Lawrence RL, Ruder MC, Zauel R, Bey MJ (2020) Instantaneous helical axis estimation of glenohumeral kinematics: the impact of rotator cuff pathology. J Biomech 109:109924. https://doi.org/10.1016/j.jbiomech.2020.109924
62. Mannel H, Marin F, Claes L, Dürselen L (2004) Establishment of a knee-joint coordinate system from helical axes analysis - a kinematic approach without anatomical referencing. IEEE Trans Biomed Eng 51:1341–1347. https://doi.org/10.1109/TBME.2004.828051
63. Cescon C, Cattrysse E, Barbero M (2014) Methodological analysis of finite helical axis behavior in cervical kinematics. J Electromyogr Kinesiol 24:628–635. https://doi.org/10.1016/j.jelekin.2014.05.004
64. Colle F, Bignozzi S, Lopomo N et al (2012) Knee functional flexion axis in osteoarthritic patients: comparison in vivo with transepicondylar axis using a navigation system. Knee Surgery, Sport Traumatol Arthrosc 20:552–558. https://doi.org/10.1007/s00167-011-1604-z
65. Churchill DL, Incavo SJ, Johnson CC, Beynnon BD (1998) The transepicondylar axis approximates the optimal flexion axis of the knee. Clin Orthop Relat Res 356:111–118. https://doi.org/10.1097/00003086-199811000-00016
66. Grip H, Häger C (2013) A new approach to measure functional stability of the knee based on changes in knee axis orientation. J Biomech 46:855–862. https://doi.org/10.1016/j.jbiomech.2012.12.015
67. Blankevoort L, Huiskes R, de Lange A (1990) Helical axes of passive knee joint motions. J Biomech 23:1219–1229. https://doi.org/10.1016/0021-9290(90)90379-H
68. Thong YK, Woolfson MS, Crowe JA et al (2002) Dependence of inertial measurements of distance on accelerometer noise. Meas Sci Technol 13:1163–1172. https://doi.org/10.1088/0957-0233/13/8/301
69. Smołka J, Skublewska-Paszkowska M (2014) Comparison of interpolation methods based on real human motion data. Prz Elektrotechniczny 90(226–229):10.12915/pe.2014.10.54
70. Clément J, de Guise JA, Fuentes A, Hagemeister N (2018) Comparison of soft tissue artifact and its effects on knee kinematics between non-obese and obese subjects performing a squatting activity recorded using an exoskeleton. Gait Posture 61:197–203. https://doi.org/10.1016/j.gaitpost.2018.01.009

Andrea Ancillao received the master's degree in Clinical and Biomedical Engineering from the Sapienza University of Rome, Rome, Italy, in 2010, and the Ph.D. degree cum laude in Industrial Production Engineering in 2017 from the same university. He has several years of research experience in the field of biomechanics, functional evaluation, and design of measurement protocols for the analysis of human motion. He is currently a post-doc researcher at the KU Leuven University, Leuven, BE.